Lasers in Manufacturing Conference 2023

Manufacturing of a Fresnel axicon on a millimeter scale using two-photon polymerization

Felix Behlau[a,*] , Jan Marx[a], Cemal Esen[a], Andreas Ostendorf[a]

[a]*Applied Laser Technologies, Ruhr-Universität Bochum, Universitätsstr. 150, 44801 Bochum, Germany*

Abstract

Two-Photon Polymerization (2PP) is an additive manufacturing process capable of manufacturing arbitrary three-dimensional structures with sub-micrometer resolution, making it an ideal technology for the fabrication of custom optical elements. However, the size of the fabricated optical elements is limited by the field of view of the lens system used during manufacturing. To manufacture large optical elements on the millimeter scale, stitching of the laser paths is required. This paper presents a stitching algorithm that incrementally divides each laser path into areas equal to the field of view of the microscope objective used (500 µm x 500 µm) by calculating the intersections of the laser paths with the area boundaries. Thus, user-defined optics can be automatically fabricated area by area, resulting in millimeter scale custom optics. As a proof of concept, a 3.5 mm diameter Fresnel axicon is fabricated using 2PP. This axicon was used for generation of a ring beam, which is analyzed with a beam profiler.

Keywords: two-photon polymerization; additive manufacturing; Fresnel optics; axicon; beam shaping

1. Introduction

Additive manufacturing is a promising fabrication technology to produce optics due to its shape flexibility, which allows the production of user-defined optics. Compared to subtractive manufacturing technologies, additive manufacturing enables the fabrication of significantly more complex shapes [1]. In particular, Two-Photon Polymerization (2PP) is an ideal technology for manufacturing user-defined optics because it is the highest-resolution additive manufacturing technology [2]. 2PP enables the layer-by-layer fabrication of arbitrary 3D shapes with a resolution of individual structural elements of less than 100 nm [3]. The 2PP process uses a tightly focused ultra-short pulse laser beam to induce a photopolymerization process within a photosensitive material by absorbing two photons quasi-simultaneously [4]. The achievable surface roughness of 2PP is in the range of 15 nm, which is low enough for optical applications [5]. In addition, photosensitive materials that are transparent to the visible light spectrum are widely available. [6]. As shown in the literature, 2PP has already been used in various fields to fabricate optical elements, such as micro-optics on optical fiber tips [7], micro-lenses on CMOS image sensors [8], or collimation lenses for LEDs [9].

However, a disadvantage of 2PP in optics fabrication is the low throughput [10]. One way to reduce process time is to manufacture Fresnel optics instead of volumetric optics. Fresnel optics have significantly lower thickness than volumetric optics [11]. Thus, the number of layers required to fabricate the optical element with 2PP is substantially reduced, thereby increasing throughput.

Another disadvantage of 2PP is the limited maximum size of the fabricated optical elements due to the limited Field of View (FOV) of the microscope objective used to focus the laser beam inside the photosensitive material. Since the high resolution of the 2PP process requires a microscope objective with a large numerical aperture (NA) [12], the resulting FOV is limited, typically in the range of 150 µm x 150 µm to 500 µm x 500 µm [13 - 14]. Therefore, stitching is required for optical elements larger than the FOV. However, stitching is a time-consuming process for large optics with a diameter several times larger than the FOV of the microscope objective, as there are no programs available that are capable of automated stitching.

This work presents a stitching algorithm that enables the automated fabrication of user-defined optics by 2PP without size limitation. All laser paths generated from the Computer-Aided Design (CAD) model of the custom optics are automatically split and sorted into areas equal to the FOV of the microscope objective used. Therefore, the user-defined optics could be manufactured area by area. To verify the developed algorithm, a Fresnel axicon with a diameter of 3.5 mm was manufactured. After fabrication, the Fresnel axicon was illuminated with a laser, and the resulting ring beam was analyzed using a beam profiler.

2. Experimental setup

The Fresnel axicon presented here has a diameter of 3.5 mm and an axicon angle of 20°. The cross-section of a single Fresnel axicon segment with all dimensions is shown in Fig. 1 a). A CAD software (Inventor 2023, Autodesk, Inc.) was used to model the Fresnel axicon. A 3D image of a section from the CAD model of the Fresnel axicon is shown in Fig. 1 b).

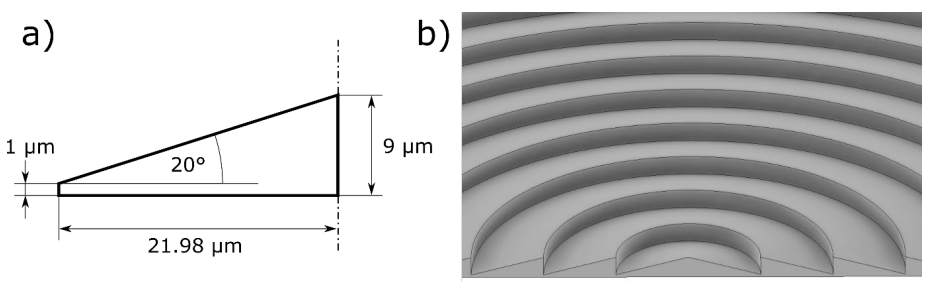

Fig. 1. (a) Cross-section of a single Fresnel axicon segment with its dimensions; (b) section view of the center of the Fresnel axicon 3D model

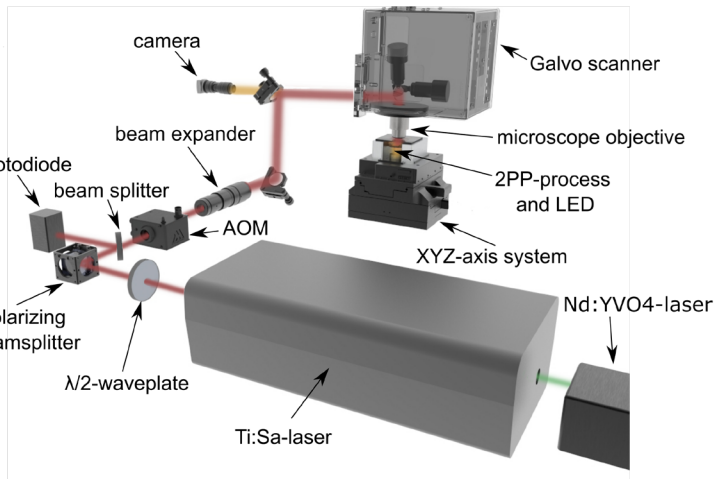

Fig. 2. Experimental Setup for the 2PP process

The 2PP setup used for manufacturing the Fresnel axicon is shown in Fig. 2. A Ti:Sa laser (Tsunami, Spectra-Physics Inc.) with a wavelength of 780 nm, a pulse width of 100 fs and a pulse repetition rate of 82 MHz was used. The average laser power was adjusted using a λ/2 - waveplate and a polarizing beam splitter cube. An acustooptic modulator (MODA110, AA Opto-Electronic) was used as a shutter. A microscope objective (20x NA=0.8 Plan-Apochromat, Carl Zeiss Microscopy Germany GmbH) with a FOV of 500 µm x 500 µm was used to focus the laser beam inside the photosensitive material. The photosensitive material used consists of 20 % zirconium propoxide and 80 % methacryloxypropil trimethoxysylane [15]. The photoinitiator used was 4,4'-Bis- (diethylamino)-benzophenon. The relative movement between the laser beam and the photosensitive material was performed by a Galvo scanner (hurrySCAN II 14, SCANLAB GmbH). Three linear axes (Wafer Max Z and ANT 130-XY, Aerotech Inc.) were used to adjust the position of the sample. The process parameters used to manufacture the Fresnel axicon are listed in Table 1.

After processing, the Fresnel axicon was illuminated with an 800 nm Ti:Sa laser (Spitfire Ace, Spectra-Physics Inc.) emitting 110 fs pulses at a repetition rate of 5 kHz. An average laser power of 2 W could be withstood by the Fresnel axicon. The resulting ring beam was analyzed with a beam profiler (LASERCAM HR, Coherent Inc.) placed 15 mm away from the Fresnel axicon.

Table 1. 2PP process parameters

Parameter	Value
Average laser power	22 mW
Laser fluence	80 mJ/cm²
Laser scan speed	300 mm/s
Layer Thickness	0.1 µm
Hatch distance	0.2 µm
Fresnel axicon diameter	3.5 mm
Microscope objective FOV	500 µm x 500 µm

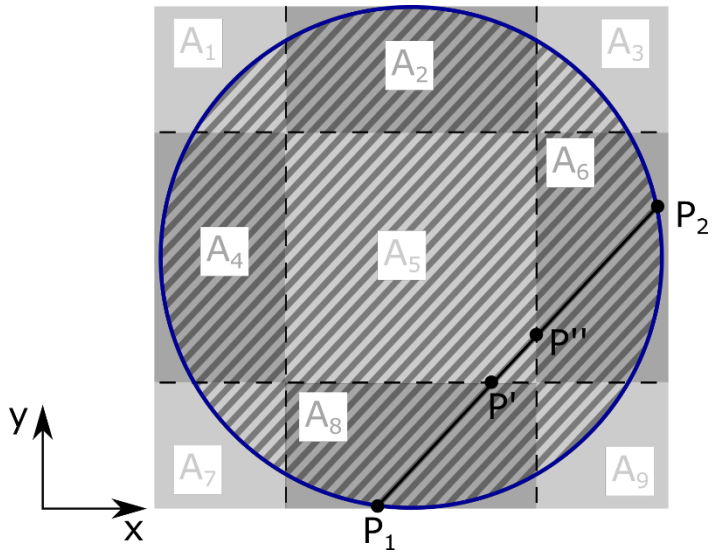

Fig. 3. Top view of a sliced layer from a circular 3D model. The contour is marked in blue and the shaded lines indicate the laser paths. The FOV areas of the microscope objective are highlighted in gray and numbered from A_1 to A_9. One laser path is highlighted in black (P_1 to P_2) and its intersections with the FOV boundaries are marked (P' and P'')

3. Automated stitching algorithm

In order to manufacture user-defined optics by 2PP a 3D CAD model is sliced into layers with laser paths that approximate the cross-section of the model. Fig. 3 shows the top view of a sliced layer from a circular 3D model. The laser paths are indicated by the shaded lines and one laser path is shown as an example (P_1 to P_2). The areas corresponding to the FOV of the microscope objective used are shown in gray and are numbered from A_1 to A_9. To manufacture the shown model by stitching, all laser paths must be split at the boundaries of the FOV areas A_i. The resulting sub-paths must be sorted into the corresponding area to ensure that every area contains all required laser paths. Thus, all areas can be processed one after the other. To calculate all intersections with the FOV boundaries and to sort all sub-paths, an iterative algorithm was developed to split the laser paths incrementally from intersection to intersection. This approach was chosen because there are too many ways in which a laser path can be positioned relative to the FOV boundaries to develop a generic algorithm that covers all cases. The algorithm for sorting and splitting a laser path is described in the following steps and the corresponding flowchart is shown in Fig 4.

First, the total number of areas A_i is calculated by dividing the size of the CAD model by the size of the microscope objective FOV in the x- and y-direction. A list is created for each area A_i, to store all split laser paths sorted by their corresponding area. A loop is initiated at this point for each layer of the model until no more layers remain. Within each layer, another loop is initiated to process each laser path contained within that layer. These nested loops ensure the execution of the subsequent splitting algorithm for each laser path within each layer.

The algorithm proceeds by calculating the number of intersections n and the direction vector for the current laser path. The coordinates of the start point (P_1 in the example) and end point (P_2 in the example) of each laser path are known from the slicing process. By determining the FOV area in which P_1 and P_2 are located, the number of intersections between the laser path and the FOV boundaries can be calculated. The end point P_2 is located one FOV area adjacent to the FOV area of P_1 in positive x-direction and one FOV area adjacent to

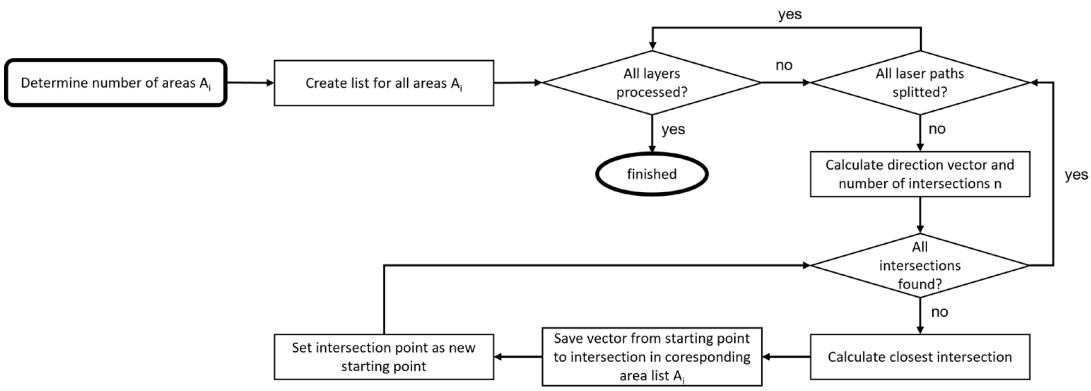

Fig. 4. Flowchart of the splitting and sorting algorithm for all laser paths to enable automated stitching

the FOV area of P_1 in the positive y-direction. Therefore, in this example, two intersection points must be calculated because the total number of intersection points is the sum of the areas passed in the x- and y-directions. However, if an area is intersected exactly at one of its corners, the number of intersection points to be determined is reduced by one. This case can be identified by the appearance of two identical intersection points. In addition, the direction vector of the laser path can be calculated from the start and end point coordinates. Knowing the direction vector is essential to determine whether the next intersection point should be found in the positive or negative x- and y-directions relative to the start point.

At this point, another loop starts until all intersection points n are found. The next possible intersection points are determined by calculating the intersection of the laser path with the area boundaries. In Fig. 3, for instance, these two intersection points are P’ and P’’. Calculating the distance between the starting point P_1 and the intersection points P’ and P’’ determines the closest intersection. The vector between the start point and the closest intersection point (P_1 - P’) is stored in the list of the corresponding area (A_8). The intersection point P’ is set as the start point for the next iteration and the algorithm is repeated until all the intersection points are found.

As a result, the optical element can be manufactured area by area once all the laser paths have been split and sorted. In this case, the axis system is used to position the sample in the center of area A_1. The Galvo scanner is used to move the laser beam through the photosensitive material along all the laser paths stored in the list for area A_1. This is done layer-by-layer, with each layer being positioned by the z-axis of the axis system. When each layer of an area is completed, the axis system positions the sample in the center of the next area until all areas are completed.

4. Results

Fig. 5 a) shows a light microscope image of the Fresnel axicon at 2.5x magnification. The Fresnel axicon has a diameter of 3.5 mm and its segments have a size of 500 µm x 500 µm. The complete Fresnel axicon was manufactured in 35 h. In the image, small gaps can be observed between the FOV areas. The width of these gaps was measured to be 3.8 µm with a standard deviation of 1.7 µm. In addition, a small hole is visible in the upper left quarter of the Fresnel axicon, which may have been caused by a dust particle adhering to the glass substrate before the photoresist was applied.

A scanning electron microscope (SEM) image of the Fresnel axicon at 2500x magnification is shown in Fig. 5 b). The image was taken at an angle of 45° relative to the Fresnel axicon and centered around a FOV area

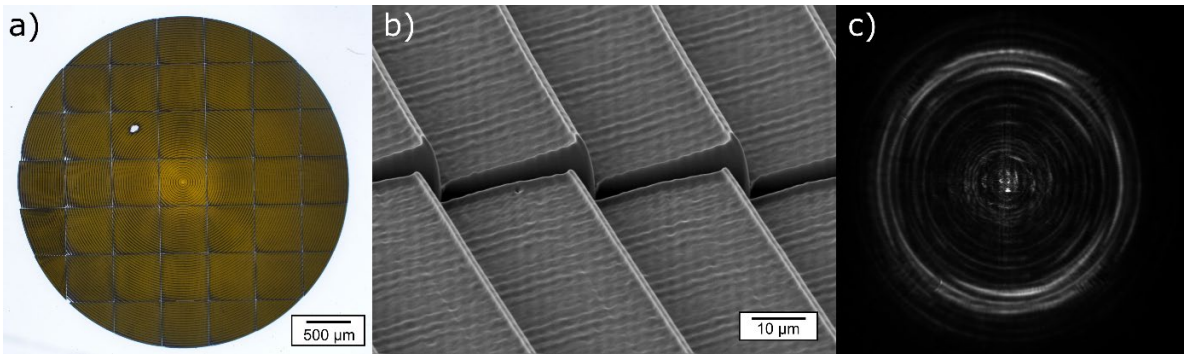

Fig. 5. (a) Light microscope image of the 3.5 mm diameter Fresnel Axicon at 2.5x magnification; (b) 45° angled SEM image of the FOV boundary at 2500x magnification; (c) beam profiler image behind the Fresnel axicon illuminated by an 800 nm laser

boundary. Due to the angled orientation of the image, a small offset between the two areas can be observed. Furthermore, the surface exhibits a slightly wavy structure due to the limited process resolution caused by the NA value of the microscope objective. While the relatively low NA value of 0.8 enables a working area of 500 µm x 500 µm, it also limits the process resolution.

Fig. 5 c) shows the beam profiler image of the laser beam obtained after illuminating the Fresnel axicon. The image clearly demonstrates the successful generation of a ring-shaped beam. Furthermore, the presence of higher-order ring maxima, which are characteristic features of Fresnel axicons [16], can be observed. In addition, small spots appear in the center of the ring, most likely due to the gaps between the regions.

5. Conclusion

In this paper, it was successfully demonstrated how an automated stitching algorithm enables the fabrication of custom optics with a diameter exceeding the FOV of the microscope objective used. Specifically, a 3.5 mm diameter Fresnel axicon was manufactured and its beam shaping properties were successfully verified. The stitching algorithm used an iterative approach, automatically splitting and organizing the laser paths into areas matching the FOV of the microscope objective. This allows the user-defined optics to be manufactured area by area.

By manufacturing Fresnel optics instead of volumetric optics, the 2PP process achieved reasonable process times for manufacturing millimeter-scale optics. This advantage is due to the significantly lower thickness of Fresnel optics compared to volumetric optics, resulting in fewer layers required. In addition, the use of a microscope objective with an NA value of 0.8 enables a FOV of 500 µm x 500 µm to reduce the number of areas required compared to microscope objectives with a higher NA value. However, using a higher NA objective would increase the process resolution to minimize the surface roughness, but at the expense of a smaller FOV, which increases the number of areas required and therefore the process time. Furthermore, the stitching process can be further improved by adjusting the scaling of the individual areas to minimize the size of the gaps between them. These two measures have the potential to further improve the light intensity distribution.

Acknowledgements

The authors thank the German Federal Ministry of Education and Research (BMBF) for financial support of this project (FKZ: 03VP09211, MINI2PP).

References

[1] A. Zolfaghari, T. Chen, A.Y. Yi, Additive manufacturing of precision optics at micro and nanoscale, Int. J. Extrem. Manuf. 1 (2019) 12005. https://doi.org/10.1088/2631-7990/ab0fa5.

[2] Q. Geng, D. Wang, P. Chen, S.-C. Chen, Ultrafast multi-focus 3-D nano-fabrication based on two-photon polymerization, Nature communications 10 (2019) 2179. https://doi.org/10.1038/s41467-019-10249-2.

[3] X. Zhou, Y. Hou, J. Lin, A review on the processing accuracy of two-photon polymerization, AIP Advances 5 (2015) 30701. https://doi.org/10.1063/1.4916886.

[4] H. Wang, W. Zhang, D. Ladika, H. Yu, D. Gailevičius, H. Wang, C.-F. Pan, P.N.S. Nair, Y. Ke, T. Mori, J.Y.E. Chan, Q. Ruan, M. Farsari, M. Malinauskas, S. Juodkazis, M. Gu, J.K.W. Yang, Two-Photon Polymerization Lithography for Optics and Photonics: Fundamentals, Materials, Technologies, and Applications, Adv Funct Materials (2023) 2214211. https://doi.org/10.1002/adfm.202214211.

[5] J. Li, P. Fejes, D. Lorenser, B.C. Quirk, P.B. Noble, R.W. Kirk, A. Orth, F.M. Wood, B.C. Gibson, D.D. Sampson, R.A. McLaughlin, Two-photon polymerisation 3D printed freeform micro-optics for optical coherence tomography fibre probes, Scientific reports 8 (2018) 14789. https://doi.org/10.1038/s41598-018-32407-0.

[6] L. Jonušauskas, D. Gailevičius, L. Mikoliūnaitė, D. Sakalauskas, S. Šakirzanovas, S. Juodkazis, M. Malinauskas, Optically Clear and Resilient Free-Form μ-Optics 3D-Printed via Ultrafast Laser Lithography, Materials (Basel, Switzerland) 10 (2017). https://doi.org/10.3390/ma10010012.

[7] C. Xiong, C. Liao, Z. Li, K. Yang, M. Zhu, Y. Zhao, Y. Wang, Optical Fiber Integrated Functional Micro-/Nanostructure Induced by Two-Photon Polymerization, Front. Mater. 7 (2020). https://doi.org/10.3389/fmats.2020.586496.

[8] S. Thiele, K. Arzenbacher, T. Gissibl, H. Giessen, A.M. Herkommer, 3D-printed eagle eye: Compound microlens system for foveated imaging, Science advances 3 (2017) e1602655. https://doi.org/10.1126/sciadv.1602655.

[9] S. Thiele, T. Gissibl, H. Giessen, A.M. Herkommer, Ultra-compact on-chip LED collimation optics by 3D femtosecond direct laser writing, Optics letters 41 (2016) 3029–3032. https://doi.org/10.1364/ol.41.003029.

[10] H. Kim, S.K. Saha, Defect control during femtosecond projection two-photon lithography, Procedia Manufacturing 48 (2020) 650–655. https://doi.org/10.1016/j.promfg.2020.05.157.

[11] M. Ali, F. Alam, H. Butt, Fabrication of 5D Fresnel Lenses via Additive Manufacturing, ACS materials Au 2 (2022) 602–613. https://doi.org/10.1021/acsmaterialsau.2c00026.

[12] V.F. Paz, M. Emons, K. Obata, A. Ovsianikov, S. Peterhänsel, K. Frenner, C. Reinhardt, B. Chichkov, U. Morgner, W. Osten, Development of functional sub-100 nm structures with 3D two-photon polymerization technique and optical methods for characterization, Journal of Laser Applications 24 (2012) 42004. https://doi.org/10.2351/1.4712151.

[13] M. Pisanello, Di Zheng, A. Balena, F. Pisano, M. de Vittorio, F. Pisanello, An open source three-mirror laser scanning holographic two-photon lithography system, PloS one 17 (2022) e0265678. https://doi.org/10.1371/journal.pone.0265678.

[14] D.E. Marschner, S. Pagliano, P.-H. Huang, F. Niklaus, A methodology for two-photon polymerization micro 3D printing of objects with long overhanging structures, Additive Manufacturing 66 (2023) 103474. https://doi.org/10.1016/j.addma.2023.103474.

[15] A. Ovsianikov, J. Viertl, B. Chichkov, M. Oubaha, B. MacCraith, I. Sakellari, A. Giakoumaki, D. Gray, M. Vamvakaki, M. Farsari, C. Fotakis, Ultra-low shrinkage hybrid photosensitive material for two-photon polymerization microfabrication, ACS nano 2 (2008) 2257–2262. https://doi.org/10.1021/nn800451w.

[16] K. Gourley, I. Golub, B. Chebbi, Demonstration of a Fresnel axicon, Applied optics 50 (2011) 303–306. https://doi.org/10.1364/AO.50.000303.